



Article

Evaluation of Ouabain's Tissue Distribution in C57/Black Mice Following Intraperitoneal Injection, Using Chromatography and Mass Spectrometry

Denis A. Abaimov ¹, Rogneda B. Kazanskaya ^{1,2}, Ruslan A. Ageldinov ³, Maxim S. Nesterov ³, Yulia A. Timoshina ^{1,4}, Angelina I. Platova ⁵, Irina J. Aristova ^{2,6}, Irina S. Vinogradskaya ⁷, Tatiana N. Fedorova ¹, Anna B. Volnova ^{2,6}, Raul R. Gainetdinov ^{6,8} and Alexander V. Lopachev ^{1,6,*}

- ¹ Research Center of Neurology, Volokolamskoye Shosse 80, 125367 Moscow, Russia; abaimov@neurology.ru (D.A.A.); timoshina.yu.a@neurology.ru (Y.A.T.); fedorova@neurology.ru (T.N.F.)
 - ² Biological Department, Saint Petersburg State University, Universitetskaya Emb. 7/9, 199034 St. Petersburg, Russia; aristovy@hotmail.com (I.J.A.); a.volnova@spbu.ru (A.B.V.)
 - ³ Scientific Center for Biomedical Technologies of the Federal Biomedical Agency of Russia, 119435 Krasnogorsk, Russia; ageldinov@gmail.com (R.A.A.); mdulya@gmail.com (M.S.N.)
 - ⁴ Biological Department, Lomonosov Moscow State University, Leninskiye Gory 1, 119991 Moscow, Russia
 - ⁵ The Mental Health Research Center, Kashirskoye Shosse 34, 115522 Moscow, Russia; platova@psychiatry.ru
 - ⁶ Institute of Translational Biomedicine, Saint Petersburg State University, Universitetskaya Emb. 7/9, 199034 St. Petersburg, Russia; gainetdinov.raul@gmail.com
 - ⁷ Non-State Private Educational Institution of Higher Professional Education, Moscow University for Industry and Finance "Synergy", Meshchanskaya Street, 9/14, Building 1, 129090 Moscow, Russia; irina_www@mail.ru
 - ⁸ Saint-Petersburg University Hospital, 199034 St. Petersburg, Russia
- * Correspondence: lopsasha@yandex.ru



Citation: Abaimov, D.A.; Kazanskaya, R.B.; Ageldinov, R.A.; Nesterov, M.S.; Timoshina, Y.A.; Platova, A.I.; Aristova, I.J.; Vinogradskaya, I.S.; Fedorova, T.N.; Volnova, A.B.; et al. Evaluation of Ouabain's Tissue Distribution in C57/Black Mice Following Intraperitoneal Injection, Using Chromatography and Mass Spectrometry. *Int. J. Mol. Sci.* **2024**, *25*, 4318. <https://doi.org/10.3390/ijms25084318>

Academic Editors: Olga V. Fedorova, Alexei Y. Bagrov and Anastasios Lymperopoulos

Received: 28 February 2024

Revised: 1 April 2024

Accepted: 10 April 2024

Published: 13 April 2024



Copyright: © 2024 by the authors. Licensee MDPI, Basel, Switzerland. This article is an open access article distributed under the terms and conditions of the Creative Commons Attribution (CC BY) license (<https://creativecommons.org/licenses/by/4.0/>).

Abstract: Cardiotonic steroids (CTSs), such as digoxin, are used for heart failure treatment. However, digoxin permeates the brain–blood barrier (BBB), affecting central nervous system (CNS) functions. Finding a CTS that does not pass through the BBB would increase CTSs' applicability in the clinic and decrease the risk of side effects on the CNS. This study aimed to investigate the tissue distribution of the CTS ouabain following intraperitoneal injection and whether ouabain passes through the BBB. After intraperitoneal injection (1.25 mg/kg), ouabain concentrations were measured at 5 min, 15 min, 30 min, 1 h, 3 h, 6 h, and 24 h using HPLC–MS in brain, heart, liver, and kidney tissues and blood plasma in C57/black mice. Ouabain was undetectable in the brain tissue. Plasma: $C_{max} = 882.88 \pm 21.82$ ng/g; $T_{max} = 0.08 \pm 0.01$ h; $T_{1/2} = 0.15 \pm 0.02$ h; $MRT = 0.26 \pm 0.01$. Cardiac tissue: $C_{max} = 145.24 \pm 44.03$ ng/g (undetectable at 60 min); $T_{max} = 0.08 \pm 0.02$ h; $T_{1/2} = 0.23 \pm 0.09$ h; $MRT = 0.38 \pm 0.14$ h. Kidney tissue: $C_{max} = 1072.3 \pm 260.8$ ng/g; $T_{max} = 0.35 \pm 0.19$ h; $T_{1/2} = 1.32 \pm 0.76$ h; $MRT = 1.41 \pm 0.71$ h. Liver tissue: $C_{max} = 2558.0 \pm 382.4$ ng/g; $T_{max} = 0.35 \pm 0.13$ h; $T_{1/2} = 1.24 \pm 0.7$ h; $MRT = 0.98 \pm 0.33$ h. Unlike digoxin, ouabain does not cross the BBB and is eliminated quicker from all the analyzed tissues, giving it a potential advantage over digoxin in systemic administration. However, the inability of ouabain to pass through the BBB necessitates intracerebral administration when used to investigate its effects on the CNS.

Keywords: cardiotonic steroids; brain–blood barrier; ouabain; digoxin; brain; blood plasma; kidney; cardiac tissue; liver

1. Introduction

Cardiotonic steroids (CTSs), commonly called cardiac glycosides, are a group of compounds used for treating heart failure. They are primarily found in plants, such as digitalis, although mammals also possess endogenous CTSs [1]. CTSs are composed of a steroidal core and a lactone ring and may include 1–3 monosaccharide residues. CTSs, as a whole, can be subdivided into two groups based on the number of carbon atoms in the lactone ring: cardenolides (5-carbon lactone ring) and bufadienolides (6-carbon lactone ring).

The pharmacological target of CTSs is the Na^+/K^+ -ATPase (NKA) enzyme, which has a CTS-binding pocket in its extracellular section. CTS binding causes NKA inhibition and activates a number of intracellular signaling pathways, including MAPK [2,3]. In the heart, this can cause cardiac muscular hypertrophy [4,5].

However, although low concentrations of the CTS digoxin are used for treating heart failure [6], because of its positive inotropic effect, the applicability of CTSs in the clinic is limited by their adverse side effects, including those on the central nervous system (CNS). Some of the CNS side effects include headaches, dizziness, brain fog, sleep disturbances, and delirium [7,8]. The prevalence of these side effects is mediated by the permeability of the blood–brain barrier (BBB) to most CTSs.

Ouabain, like digoxin, is a cardenolide. However, unlike digoxin, ouabain has a CH_2OH group at the C10 position, hydroxyl groups at C1 and C5, and rhamnose, increasing its polarity (Figure 1). Studies utilizing the direct intracerebroventricular administration of the CTS ouabain to rats and mice demonstrated that CTSs can cause changes in dopaminergic signaling, accompanied by mania-like behaviors [9,10]. As the BBB is known to be permeable primarily to lipophilic molecules, the increased polarity of ouabain compared to other CTSs suggests that it will not pass through the BBB as easily. This makes ouabain interesting as a potential alternative to digoxin in treating patients. Previously, ouabain has been applied in clinical practice in Germany under the trademark “Strodival” (Meda Pharma GmbH, Solna, Sweden). However, its use in Germany was discontinued in 2006. At the present moment, ouabain is clinically used only in Ukraine, where it is registered as “Strophantin-G”.

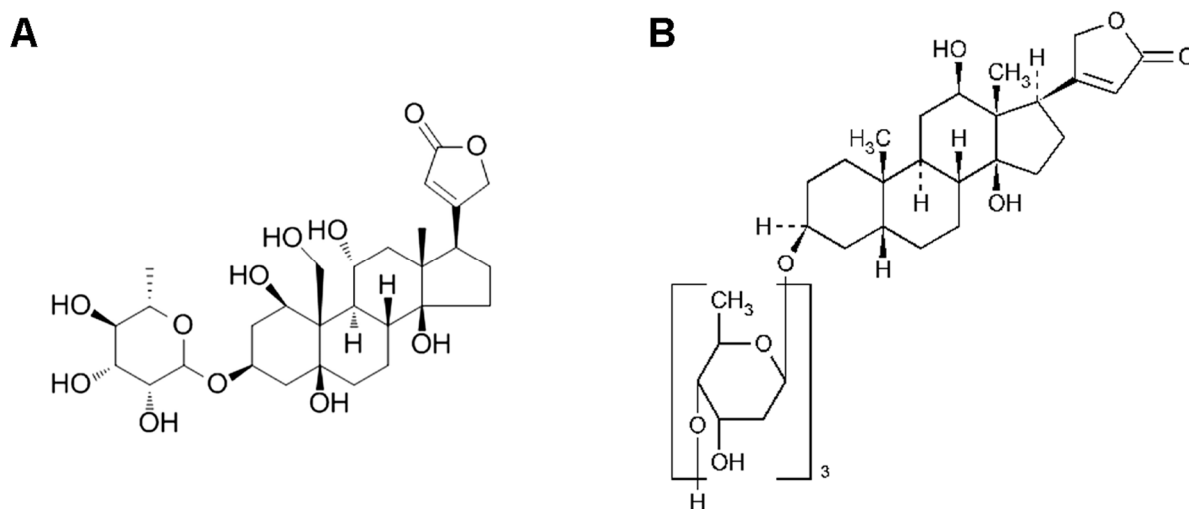


Figure 1. Structures of the CTS ouabain (A) and digoxin (B).

It is known that the pharmacokinetics of a given drug are significantly affected by the administration route. As such, the adsorption and excretion of ouabain when administered in different ways has been extensively investigated. Peroral and sublingual administration routes were shown to be ineffective, with ouabain’s enteral adsorption barely approaching 7% at 5 h post administration [11]. Absorption coefficients for peroral administration are reported to range from 0.7% to 3.0% (2.2% on average). A comparison of ouabain’s kidney excretions after intravenous and peroral administrations, using radioimmunoassays, showed that the intravenous route is superior, with kidney excretion post i.v. administration being 66% of the initial dose, while excretion post peroral administration was only 1.3% of the initial dose [12]. When ouabain is administered intravenously, its pharmacokinetics are best described using the two-compartment model. Ouabain plasma concentrations drop rapidly post injection, with its half-life in the alpha-phase reportedly ranging from 2 to 20 min. This makes evaluating the beta-phase half-life difficult, as ouabain concentrations

during it are close to undetectable. As such, its half-life in the beta-phase varies from 11 to 50 h [13].

Most investigations conducted on the pharmacokinetics of ouabain, both in animals and humans, were performed in the time period 1970–1980 and used tritium-labeled ouabain and radioisotopic detection methods, which are unable to exclude potentially pharmacologically inactive metabolites from the total measured radiation. As mentioned above, ouabain is more polar than other CTSs, making it the most likely to be resistant to passing through the blood–brain barrier. As such, it is possible that the previous studies showing the penetration of ouabain in brain tissue obtained false positives. Contemporary pharmacological evaluations of compounds of interest frequently use chromatography and mass spectrometry, which are more specific and possess fewer limitations in comparison to radioisotopic detection. Thus, investigating the ability of ouabain to penetrate the BBB, its kinetics in blood plasma, and its distribution in organs, using HPLC–MS, became the goal of this study.

This study investigated the distribution and elimination kinetics of ouabain in plasma as well as in heart, kidney, and liver tissues, using a direct HPLC–MS method rather than radioactive labeling as in earlier studies. The tropicity and bioavailability of ouabain with respect to various organs and tissues differ significantly from those of digoxin. Most importantly, we showed that ouabain does not pass through the BBB, meaning that it lacks CNS side effects when administered systemically. This, in conjunction with ouabain's tropism in cardiac tissue and lack of cardiac muscular hypertrophy induction, suggests that ouabain may be preferable to digoxin in clinical applications.

2. Results

To facilitate accurate ouabain detection, we developed a custom high-efficiency liquid chromatography–mass spectrometry (HPLC–MS) protocol, as described in the Materials and Methods section. Ouabain concentrations were evaluated in the blood plasma and brain, heart, liver, and kidney tissues of C57/black mice at a range of time-points post intraperitoneal injection of 1.25 milligrams of ouabain per kilogram of bodyweight (5 min, 15 min, 30 min, 1 h, 3 h, 6 h, and 24 h).

In the blood plasma, the maximum concentration (C_{\max}) of the ouabain was 882.88 ± 21.82 ng/g ($T_{\max} = 5$ min post injection and 0.08 ± 0.01 h). After peaking at 5 min, it decreased monoexponentially (Figure 2A), dropping to 14 ng/g at 1 h post injection. The half-life ($T_{1/2}$) of the ouabain in the plasma was determined at 0.15 ± 0.02 h. The mean retention time (MRT) was 0.26 ± 0.01 h. In sum, this implies that within 1 h following the intraperitoneal injection, ouabain almost entirely ceases circulation in the blood plasma of animals (Figure 2A). Other pharmacokinetic parameters for ouabain elimination from blood plasma are provided in Table 1.

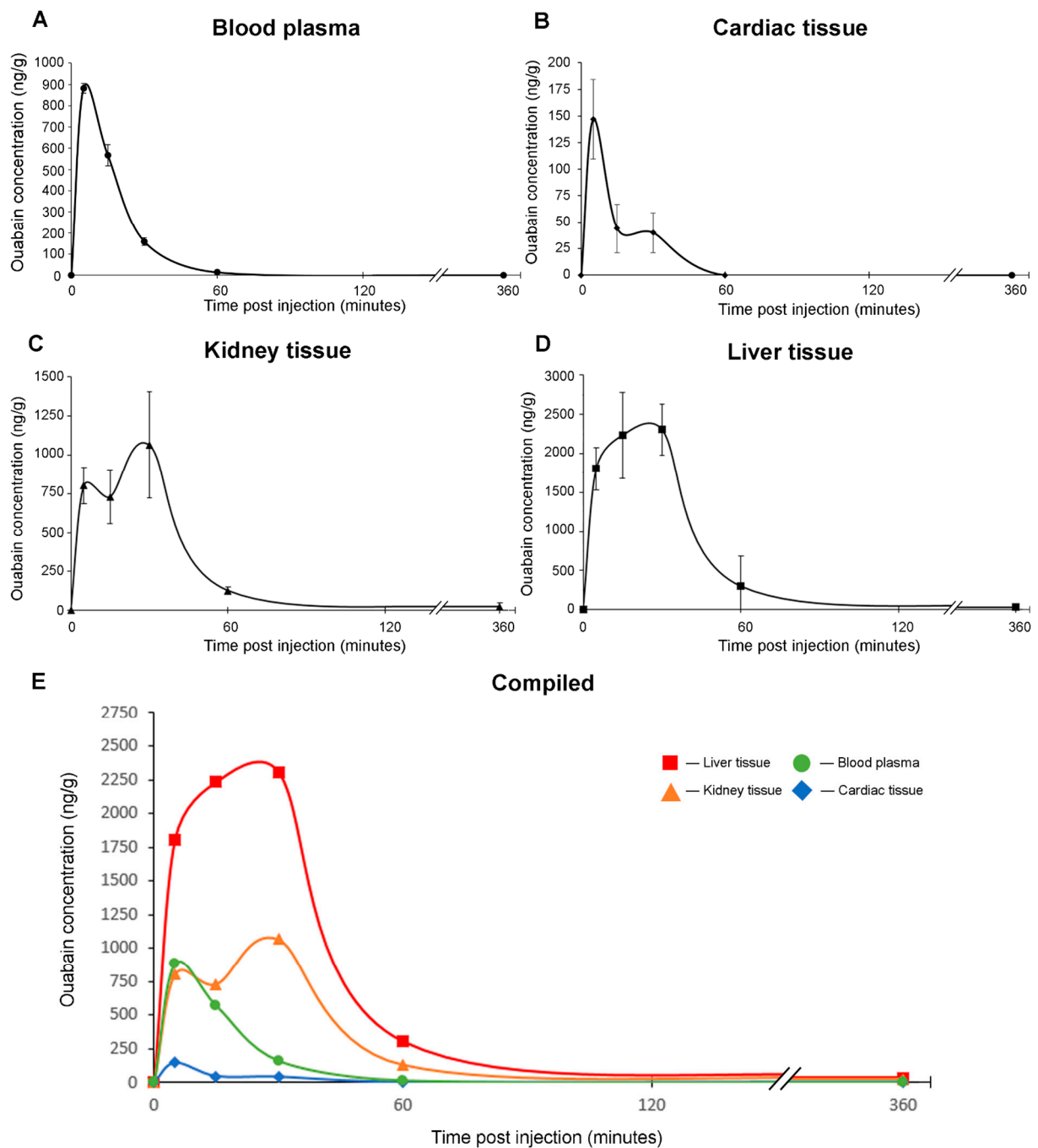


Figure 2. Averaged pharmacokinetic curves representing the elimination of ouabain from (A) blood plasma, (B) cardiac tissue, (C) kidney tissue, and (D) liver tissue following intraperitoneal injection of ouabain at a dose of 1.25 mg/kg bodyweight to C57/black mice. All the curves are superimposed in (E). X-axis—time from injection (min); y-axis—concentration (ng/g); $n = 6$. All the concentrations are presented as mean \pm SD. Error bars were omitted in (E) to increase readability.

Table 1. Pharmacokinetic parameters of ouabain in tissues after intraperitoneal injection of 1.25 mg/kg bodyweight. Pharmacokinetic parameters included C_{\max} —peak plasma concentration, T_{\max} —time of peak plasma concentration, AUC—area under the concentration–time curve (trapezoidal rule), $T_{1/2}$ —the terminal elimination half-life, V_z —volume of distribution, CL/F —apparent clearance, λ_z —terminal elimination rate constant, and mean residence time (MRT). To assess the efficiency of the drug penetration in tissues, the tissue-to-plasma partition coefficient (F_t/p , the ratio of the AUCs between the respective peripheral site and the plasma) was used. Values are expressed as mean \pm SD.

Tissue	C_{\max} , ng/g	T_{\max} , h	AUC_t , ng \times h/g	AUC_{inf} , ng h/g	MRT, h	$T_{1/2}$, h	V_z/F , g/kg	CL/F , g/kg/h	λ_z , h^{-1}	F_t/p
Brain	–	–	–	–	–	–	–	–	–	–
Blood Plasma	882.9 \pm 21.8	0.08 \pm 0.01	290.8 \pm 14.9	294.3 \pm 14.6	0.26 \pm 0.01	0.15 \pm 0.02	900 \pm 153	4259 \pm 214	4.85 \pm 0.8	1.00
Cardiac	145.2 \pm 44.0	0.08 \pm 0.02	34.4 \pm 8.7	47.6 \pm 12.9	0.38 \pm 0.14	0.23 \pm 0.09	9463 \pm 3481	29144 \pm 7223	3.42 \pm 1.29	0.12
Kidney	1072.3 \pm 260.8	0.35 \pm 0.19	872.0 \pm 132.6	939.1 \pm 145.4	1.41 \pm 0.71	1.32 \pm 0.76	2583 \pm 1321	1402 \pm 229	0.68 \pm 0.36	3.00
Liver	2558.0 \pm 382.4	0.35 \pm 0.13	2084.6 \pm 389.5	2207.6 \pm 338.8	0.98 \pm 0.33	1.24 \pm 0.7	1043 \pm 564	584 \pm 97	0.7 \pm 0.44	7.17

In the perfused brain tissue, ouabain was not detectable at any time points after the injection. As such, it can be concluded that ouabain does not pass through the BBB when administered systemically to mice and does not accumulate in the brain tissue.

In the cardiac tissue, which is the “target” CTS tissue, like in the blood plasma, T_{\max} was 5 min post injection (0.08 ± 0.02 h), and $C_{\max} = 145.24 \pm 44.03$ ng/g. After 5 min, the concentration of the ouabain decreased steadily and became undetectable at 60 min (Figure 2B). $T_{1/2}$ for the cardiac tissue was 0.23 ± 0.09 h, and MRT was 0.38 ± 0.14 h. Other pharmacokinetic parameters for ouabain elimination from the cardiac tissue are provided in Table 1. Thus, ouabain is present in animal cardiac tissue for the same amount of time following injection as in the blood plasma and does not appear to accumulate.

In the kidney tissue, C_{\max} was 1072.3 ± 260.8 ng/g, and T_{\max} was 0.35 ± 0.19 h (Figure 2C). $T_{1/2}$ was 1.32 ± 0.76 h, and MRT was 1.41 ± 0.71 h. Other pharmacokinetic parameters for ouabain elimination from the kidney tissue are provided in Table 1. In the liver tissue, the C_{\max} of the ouabain was 2558.0 ± 382.4 ng/g at 30 min post injection ($T_{\max} = 0.35 \pm 0.13$ h) (Figure 2D). $T_{1/2}$ was 1.24 ± 0.7 h, and MRT was 0.98 ± 0.33 h. Other pharmacokinetic parameters for ouabain elimination from the liver tissue are provided in Table 1. In conclusion, ouabain accumulates in both kidney and liver tissues, which is expected as they are both organs of elimination. The greater retention time of the ouabain by the liver tissue in comparison to the blood plasma indicates that the liver is the main accumulation site (Figure 2C,D).

3. Discussion

In this study, we used a custom HPLC–MS protocol to evaluate ouabain elimination from C57/black mice tissues following intraperitoneal injection (1.25 mg/kg bodyweight). In this study, we express the concentration values in nanograms of ouabain per gram of tissue, which affects our interpretation of the volumetric distribution (V_d) and clearance (CL) values. although V_d is usually expressed in liters or liters per kilogram, and CL is expressed in liters per hour or liters per hour per kilogram, in our study, V_d should be interpreted as the hypothetical mass of a test tissue in which the administered dose of the drug could be distributed to achieve the same concentration level in that test tissue.

Ouabain’s V_d/F value for plasma was 900 ± 153 g/kg. That is, the hypothetical volume of the test tissue to achieve the concentration measured in that tissue when the

same dose is administered would have to be about 900 grams per kilogram of bodyweight. In other words, this is the fraction of the volume that would be taken up by the administered substance to achieve the concentrations obtained if the entire body of the animal were represented only by the test tissue. We found that in the blood plasma, the pharmacokinetics of the ouabain are best described using a one-compartment model. After reaching its maximum during the first 5 min, the concentration of the ouabain decreases more than 10-fold within an hour, indicating that its circulation time in the plasma is relatively short. This assumption is supported by the short half-life ($T_{1/2} = 0.15 \pm 0.02$ h) and mean retention time ($MRT = 0.26 \pm 0.01$ h). This finding is consistent with previous studies performed using radioautographic methods, which indicate that ouabain is rapidly eliminated from the blood plasma within the first hour following systemic administration. In contrast, for digoxin, the MRT in the blood plasma is 10 times higher [14].

Digoxin is known to have side effects on the CNS in patients treated for heart failure [15]. According to Andersson et al., the concentration of digoxin in the brains of inpatients regularly taking digoxin can reach a level of 32 ng/g, which is comparable to that observed in skeletal muscle [16]. This elevation in the brain's digoxin concentration causes neuropsychiatric side effects, such as fatigue, depression, psychosis, and delirium [2,17]. A key finding of this study is the apparent inability of ouabain to cross the BBB in mice. This contradicts data acquired using radioautographic methods in other studies, which found trace amounts (6–7 ng/g) of ouabain in brain tissue following systemic administration [18] and is significantly higher than the lower detection threshold of our protocol. It should be noted that no previous studies have been performed specifically on mice, and making a direct comparison may be inappropriate. Rodents, including mice and rats, have adapted to a CTS-containing diet, as reflected in their CTS-resistant $\alpha 1$ NKA subunit [19]. It is possible that their BBB is also less permeable to CTS; however, digoxin does pass through the BBB of mice [14]. In cats, it was shown that most cardiac glycosides are able to cross the blood–brain barrier, with an efficiency directly proportional to their lipophilicity [20], and ouabain is less lipophilic than digoxin. Ouabain detected in the brain in previous studies may be caused by lipophilic metabolites of the radioactive-labeled ouabain, such as ouabagenin, penetrating the BBB. The investigators also may have obtained false positives due to poor cerebral perfusion and residual blood in non-perfused tissues [18]. According to our data, ouabain does not, in fact, cross the BBB readily; it could be a feasible alternative to digoxin in clinical applications.

The times of the peak drug concentration (T_{max}) in the blood plasma and cardiac tissue are almost identical (0.08 ± 0.01 h and 0.08 ± 0.02 h, respectively), indicating that ouabain rapidly perfuses the myocardium. Interestingly, although previous studies indicate that ouabain tends to accumulate in the cardiac tissue of dogs [18], we did not observe this in our experiment. One possible explanation for this phenomenon is different CTS retention patterns in rodents than in other mammals because of the presence of CTS in their diet. As mentioned above, the $\alpha 1$ NKA subunit of rodents, including rats and mice, is significantly less sensitive to CTS than that of other mammals. As such, we conjecture that the retention seen in dog cardiac tissue is related to the slower clearance of the $\alpha 1$ -subunit-bound ouabain compared to mice. It should be noted that the time of the ouabain elimination from the plasma is significantly shorter in rats than in rabbits and dogs [21], further suggesting that lower $\alpha 1$ affinity to CTS in rodents may be implicated. It is also worth noting that we found the retention time of the ouabain in the mouse cardiac tissue to be shorter than the retention time of the 3H -digoxin in the mouse cardiac tissue, as identified in an earlier study [22]. Despite shorter retention time, ouabain has an advantage over digoxin in heart failure treatment by preventing cardiac tissue hypertrophy [4,23,24].

We found the T_{max} values of the ouabain in both kidney and liver tissues to be approximately 20 min, which is 15 min more than T_{max} for the plasma and cardiac tissue. They also both had higher Ft/p and C_{max} values. Thus, the distribution coefficients of ouabain were 7.17 for liver tissue and 3.0 for kidney tissue (Table 1). These data align with the assumption that both of these organs actively participate in eliminating ouabain from

the body. The $T_{1/2}$ and MRT values are slightly higher for the liver tissue (1.24 ± 0.7 h and 0.98 ± 0.33 h, respectively) than for the kidney tissue (1.32 ± 0.76 h and 1.41 ± 0.71 , respectively). The higher AUC values for the liver tissue compared to the kidney tissue may indicate the predominance of the hepatic route in the elimination of the ouabain. This is supported by the apparent clearance (CL/F) value, which is the lowest for the liver tissue (584 ± 97 g/kg/h) and is almost 3 times higher for the kidney tissue (1402 ± 229 g/kg/h). We use the clearance-to-bioavailability (CL/F) ratio because the absolute value of CL, like Vd, can only be determined when using intravenous administration. The liver, being the primary elimination pathway of the ouabain from the body, is supported by previous studies on laboratory rodents, which indicate that the main route of the elimination is through the bile [25]. The decrease in ouabain's absorption speed in the liver tissue, which we observed as the biexponential phase of the absorption in the pharmacokinetic curve (seen as a "flat top" in Figure 2D), may be due to the saturation of active transport mechanisms, as previously shown by Kupferberg H. et al., in rat liver slices [26].

If the main elimination pathway of the ouabain is through bile secretion, we would expect its concentration to be higher in fecal matter than in urine. Unfortunately, in this study, we did not have the means to perform an evaluation of ouabain concentrations in the urine and fecal matter of the animals, so we cannot confirm this assumption. The literature data indicate that in rats, ouabain is primarily excreted in bile with little metabolism [26]. In humans, however, ouabain appears to be primarily eliminated via the kidneys [27]. The two concentration peaks observed for the kidney tissue (Figure 2C) may be an indicator of the renal tubular recirculation of the ouabain [28]. Previously, Steiness et al. [29] have shown that in humans, digoxin excretion via the urine is in equal parts due to active tubular secretion and glomerular filtration. These results were later confirmed in rats [30]. Data based on micropuncture studies have shown that ^3H -labeled digoxin in rats is absorbed from the proximal convoluted tubule but not from the loop of Henle [30]. These findings may explain the presence of two concentration peaks for the kidney tissue. In a study by Li et al. from 2021, the pharmacokinetics of the digoxin were studied in Sprague–Dawley rats, following the oral administration of the drug at a dose of $45 \mu\text{g}/\text{kg}$. The authors showed that with respect to excretory organs, digoxin exhibits liver tropism, with a peak concentration in the liver tissue of $150 \text{ ng}/\text{g}$, which is over 6 times higher than that in the kidney tissue ($22 \text{ ng}/\text{g}$) [31].

As such, we showed that ouabain does not pass through the BBB, meaning that it lacks CNS side effects when administered systemically. This should be considered when investigating the physiological effects of the ouabain, specifically on the CNS of laboratory rodents, and a direct intracerebral administration route should be used. This also implies that endogenous CTSs possessing physicochemical properties similar to those of ouabain, including polarity and structure, are unlikely to pass through the BBB in non-pathological circumstances. Also, ouabain's tropism in cardiac tissue and lack of cardiac muscular hypertrophy induction suggests that ouabain may be preferable to digoxin in clinical applications.

4. Materials and Methods

4.1. Animals

A total of 42 C57/black male mice, 3–6 months old, were used in this study. All the animals were housed under standard vivarium conditions. The day/night cycle was 12 h, and food and water were provided ad libitum. Intraperitoneal injection was used to administer ouabain at a dosage of $1.25 \text{ mg}/\text{kg}$, 3 times less than the previously published LD50 for mice ($3.75 \text{ mg}/\text{kg}$) [32]. This dose is significantly higher than therapeutic doses used for treating patients, which are 3–6 mg perorally [33,34]. After the injection, mice were sacrificed by decapitation, and the heart, kidneys, liver, brain, and blood were harvested at the following time points: 5 min, 15 min, 30 min, 1 h, 3 h, 6 h, and 24 h ($n = 6$). All the experiments were approved by the St. Petersburg State University Ethical Committee, protocol number 131-03-1 from 25 March 2019.

4.2. Sample Preparation

Ouabain was extracted from biological material using deproteinization. Tissues were homogenized in 10% trichloroacetic acid to precipitate plasma proteins. D₂-ouabain (100 ng/mL) [35] at a ratio of 1 m:2 v was added as the internal standard. The resulting suspension was ultra-centrifuged at 16,000 g to separate the denatured proteins. The supernatant was then transferred to a chromatography vial and placed in the chromatographic auto-sampler to perform further chromatography–mass spectrometry analysis.

4.3. Ouabain Detection

The ouabain concentration was measured using liquid chromatography–mass spectrometry in a Shimadzu NEXERA-XR system equipped with a Shimadzu LCMS-8040 detector, a DGU-20A5r degasser, two LC-20ADxr pumps, a SIL-20AC auto-sampler, and a CTO-20AC column thermostat with two directional flow control valves (FCV-12AH and FCV 32AH, respectively). Chromatographic separation was performed in an Aeris PEPTIDE XB-C18 (50 mm × 2.1 mm × 2.6 μm) analytical column. The mobile phase consisted of two solutions: 10 mM ammonium formate acidified with formic acid to a final concentration of 0.1% (solution A) and acetonitrile–10 mM ammonium formate (90:10) (solution B) at a ratio of 90% A:10% B acidified with formic acid to a final concentration of 0.1%. The flow speed was set to 0.45 mL/min. The sample containing the ouabain was separated using the gradient method, with a progressive increase in the content of solution B from an initial value of 5% to 90% of the total mobile phase volume during the first five minutes of the analysis, followed by a two-minute equilibration of the chromatographic column at the specified concentration level and then a return to the initial value during the next three minutes of the analysis. The injection volume was 20 μL. The separation temperature was 40 °C. The duration of the chromatography was 10 min (Figure A1).

Under these conditions, both the ouabain and D₂-ouabain (internal standard) [35] retention times constituted 3.11 ± 0.05 min. The mass-spectrometric detection of the ouabain was based on daughter ions, with m/z 439.15, 403.2, 373.2, 355.15, and 157.05, formed via the breakdown of an m/z 585.15 molecular predecessor at impact energies of 15, 16, 20, 21, and 35 eV, respectively. The second-order mass spectrum for the ouabain is presented in Figure A2.

The mass spectrometer operated in the mode of the fixation of positive ions formed by electrospray ionization (ESI). The detailed parameters of the analysis are given in Table 2. The data were processed using LabSolutions V. 5.91 software (Japan).

Table 2. Shimadzu 8040 triple quadrupole ESI interfacial parameters.

Parameter	Value	Unit
Nebulizer Gas Flow Rate	1.5	L/min
DL Temperature	250	C
Heat Block Temperature	400	C
Drying-Gas Flow Rate	15	L/min
CID Gas	230	kPa

The internal standard method was used for the quantitative measurement of the ouabain concentrations. During the calibration, the ratio of the chromatographic peak areas of the target substance and the internal standard was measured as a function of the ouabain concentration. Linear regression, based on the least-squares method, was used for the calculations. For the quantification of the ouabain, the internal standard method was used. The calibration relationship was linear over the concentration range from 5 ng/mL to 500 ng/mL (Figure A3). The concentration of the ouabain was determined using the formula $Y = 840.66 \times X$, where Y is the concentration of the analyte, expressed in ng/mL, and X is the area of the chromatographic peak of the ouabain normalized to the area of

that of the internal standard. The relative error in the method for the determination of the ouabain concentration did not exceed 10%.

4.4. Pharmacokinetic Analysis and Statistical Approach

The pharmacokinetic parameters were calculated using the noncompartmental method in the Phoenix WinNonlin 8.3 program (USA), and the statistical processing was performed in MS Office Excel. The pharmacokinetic parameters included C_{\max} —peak plasma concentration, T_{\max} —time of the peak plasma concentration, AUC—area under the concentration–time curve (trapezoidal rule), $T_{1/2}$ —the terminal elimination half-life, V —volume of the distribution, CL/F —apparent clearance, λ_z —terminal elimination rate constant, and mean residence time (MRT). To assess the efficiency of the drug penetration in the tissues, the tissue-to-plasma partition coefficient (F_t/p , the ratio of the AUCs between the respective peripheral site and the plasma) was used (Tables A1–A3). Because in mice, the estimation of an individual pharmacokinetic profile is impossible because of the small animal size (only 1 concentration measurement is possible for 1 animal), the resampling method allowed us to obtain individual PK parameters and to estimate descriptive statistics [36].

Author Contributions: Conceptualization, A.V.L. and D.A.A.; methodology, D.A.A., M.S.N., Y.A.T., I.J.A., and R.A.A.; validation, A.I.P. and I.S.V.; formal analysis, A.I.P. and M.S.N.; investigation, D.A.A., R.B.K., A.V.L., M.S.N., Y.A.T., I.J.A. and R.A.A.; resources, I.J.A., A.B.V. and A.V.L.; data curation, D.A.A. and A.I.P.; writing—original draft preparation, D.A.A. and R.B.K.; writing—review and editing, D.A.A., R.B.K., A.V.L., R.R.G., A.I.P., I.S.V. and A.B.V.; visualization, M.S.N., A.I.P., and R.B.K.; supervision, A.V.L., R.R.G. and T.N.F.; project administration, A.V.L., A.B.V., and T.N.F.; funding acquisition, A.V.L., R.R.G. and I.S.V. All authors have read and agreed to the published version of the manuscript.

Funding: This research was funded by the Russian Science Foundation, grant number 22-75-10131; the authors A.B.V. and R.R.G. acknowledge Saint Petersburg State University for a research project grant, 95444211, St. Petersburg, Russia.

Institutional Review Board Statement: The study was conducted in accordance with the Declaration of Helsinki and approved by the Ethics Committee of St. Petersburg State University (protocol code 131-03-1 from 25 March 2019).

Informed Consent Statement: Not applicable.

Data Availability Statement: The original contributions presented in this study are included in the article/Appendix A; further inquiries can be directed to the corresponding author/s. The complete raw data supporting the conclusions of this article will be made available by the authors on request.

Acknowledgments: The authors thank the Saint Petersburg State University vivarium and the Research Resource Center “Molecular and Cell Technologies” of the Research Park of the Saint Petersburg State University, Saint Petersburg, Russia for providing the facilities necessary for this study. The authors would also like to thank Olga I. Kulikova and Olga A. Muzychuk for aid with the sample preparation. The authors would also like to thank Abrek K. Sariev for aid with the data analysis.

Conflicts of Interest: The authors declare no conflicts of interest.

Appendix A

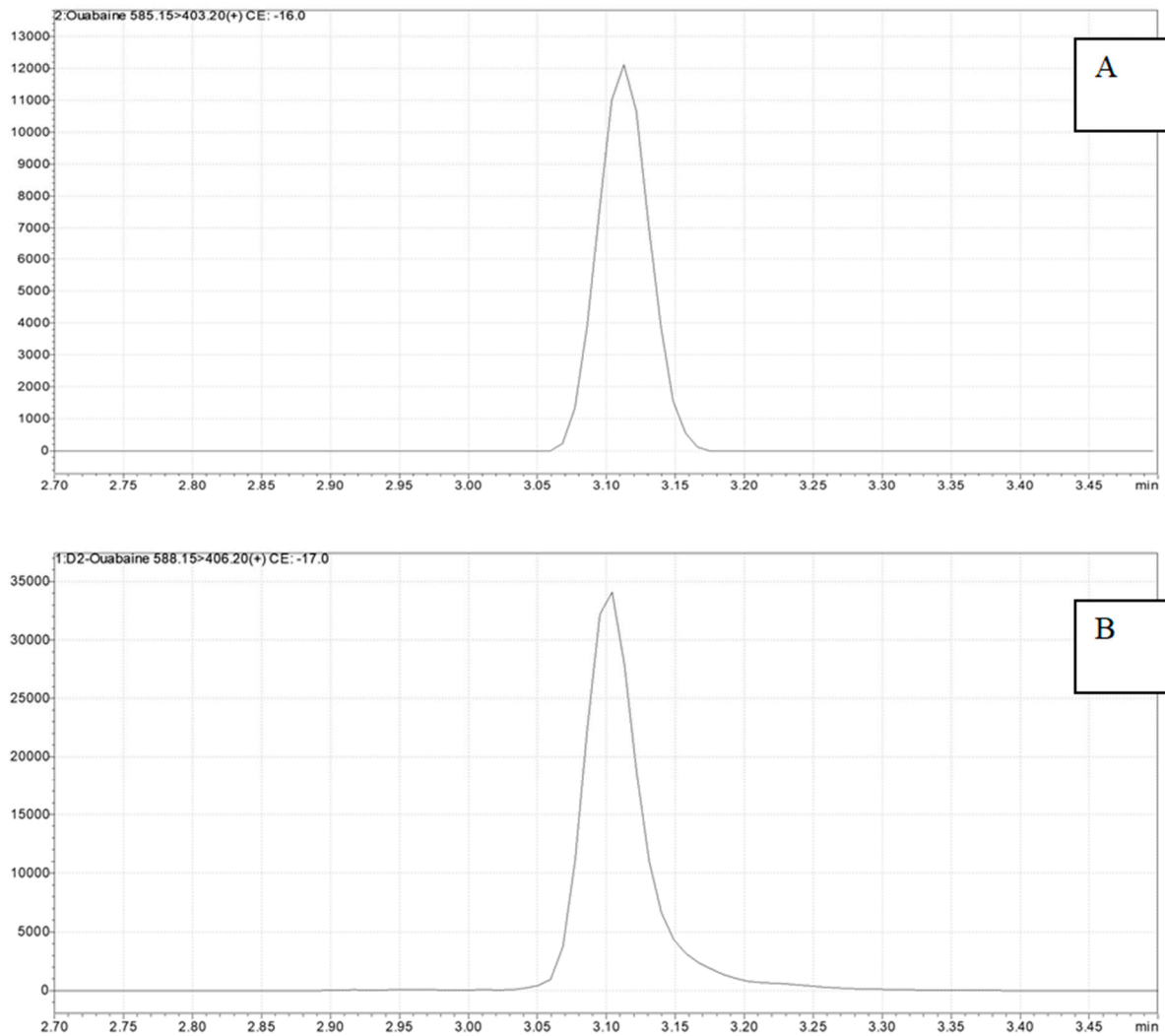


Figure A1. Demonstration chromatogram of a standard sample of ouabain (A) at a concentration of 125 ng/mL for daughter ions with m/z 403.2 and an internal standard (D₂) of ouabain at a concentration of 100 ng/mL (B) for daughter ions with m/z 376.15.

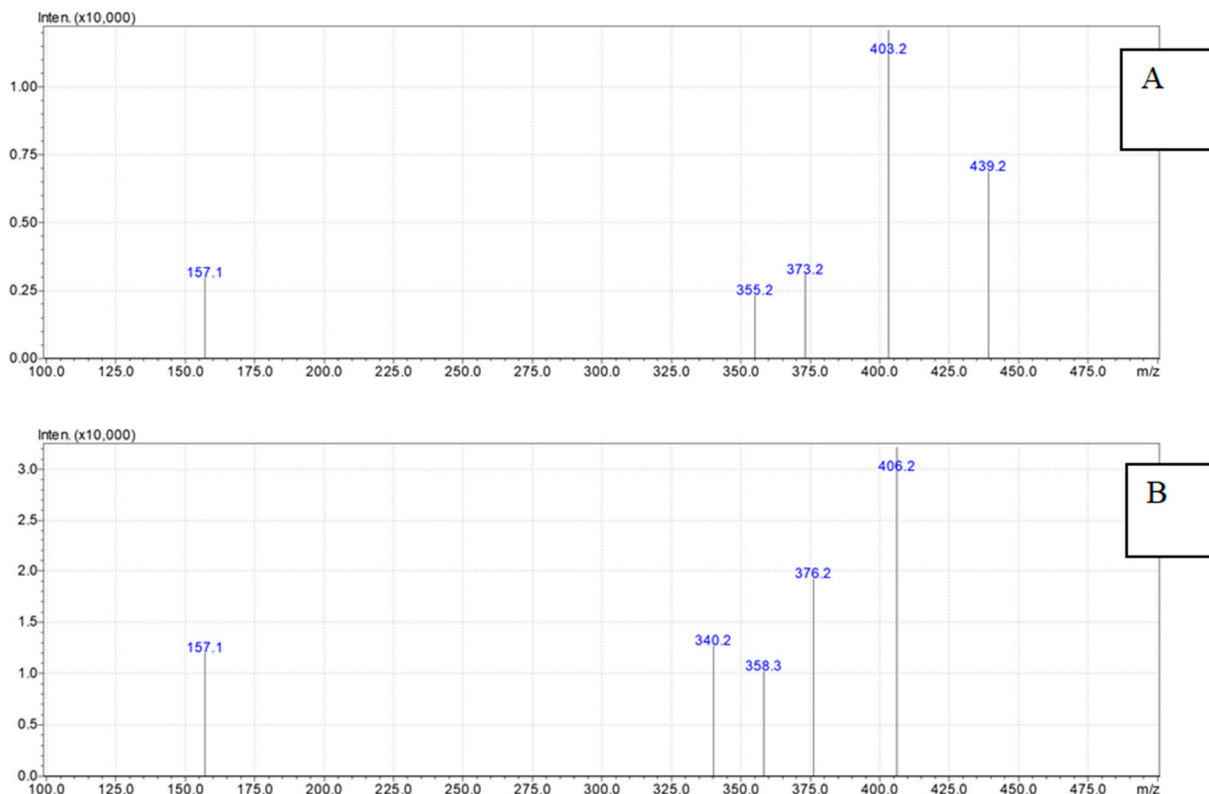


Figure A2. Second-order mass spectra for ouabain (A) and D₂-ouabain (B).

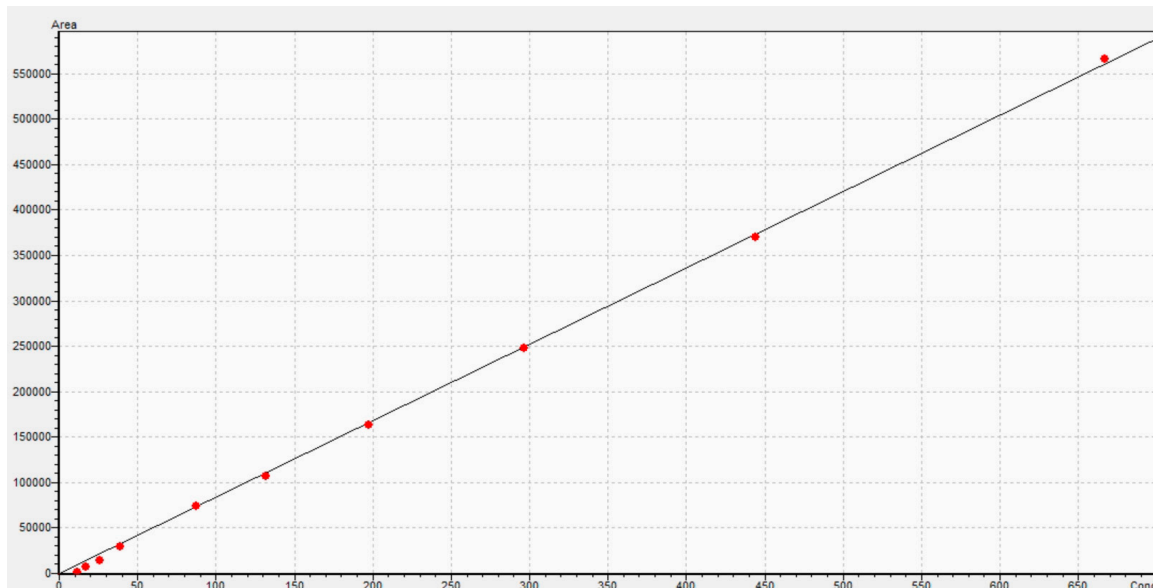


Figure A3. Calibration function of ouabain in model solutions, obtained using HPLC–MS/MS triple quadrupole method. X axis—ouabain concentration, ng/mL.

At each pharmacokinetic point, the standard deviations (SDs) were known, which made it possible to perform resampling. As a result of the resampling, 29 profiles of concentration kinetics were generated for each tissue; the first profile corresponded to actual measurements, for a total of 30 profiles, which allowed us to calculate descriptive statistics for the pharmacokinetic parameters. The following kinetic parameters were obtained from the data after resampling (Tables A1–A3).

Table A1. Pharmacokinetic parameters λ_z (h^{-1}), $T_{1/2}$ (h), and T_{max} (h) for the analyzed tissues.

Statistical Parameter	λ_z, h^{-1}				$T_{1/2}, h$				T_{max}, h			
	Cardiac	Liver	Plasma	Kidney	Cardiac	Liver	Plasma	Kidney	Cardiac	Liver	Plasma	Kidney
Mean	3.42	0.70	4.85	0.68	0.23	1.24	0.15	1.32	0.08	0.35	0.08	0.35
SD	1.29	0.44	0.80	0.36	0.09	0.70	0.02	0.76	0.00	0.13	0.00	0.19
SE	0.24	0.08	0.15	0.07	0.02	0.13	0.00	0.14	0.00	0.02	0.00	0.04
Minimum	1.49	0.16	3.81	0.15	0.10	0.26	0.10	0.49	0.08	0.25	0.08	0.08
Median	3.16	0.62	4.71	0.52	0.22	1.11	0.15	1.34	0.08	0.25	0.08	0.50
Maximum	6.68	2.68	7.00	1.41	0.47	4.27	0.18	4.58	0.08	0.50	0.08	0.50
Geometric Mean	3.19	0.63	4.79	0.60	0.22	1.11	0.15	1.16	0.08	0.33	0.08	0.27
95% Confidence Interval's Lower Limit	2.94	0.53	4.55	0.55	0.20	0.97	0.14	1.03	0.08	0.30	0.08	0.28
95% Confidence Interval's Upper Limit	3.90	0.87	5.15	0.82	0.27	1.51	0.16	1.60	0.08	0.40	0.08	0.42

Table A2. Pharmacokinetic parameters C_{max} (ng/g), AUC_t (ng \times h/g), and AUC_{inf} (ng \times h/g) for analyzed tissues.

Statistical Parameter	$C_{max}, ng/g$				$AUC_t, ng \times h/g$				$AUC_{inf}, ng \times h/g$			
	Cardiac	Liver	Plasma	Kidney	Cardiac	Liver	Plasma	Kidney	Cardiac	Liver	Plasma	Kidney
Mean	145.24	2558.00	882.88	1072.27	34.35	2084.61	290.75	871.99	47.59	2207.65	294.33	939.10
SD	44.03	382.35	21.82	260.86	8.71	389.50	14.94	132.59	12.90	338.85	14.62	145.42
SE	8.04	69.81	3.98	47.63	1.59	71.11	2.73	24.21	2.36	64.04	2.67	26.55
Minimum	81.76	1655.38	845.72	635.23	19.59	1103.55	259.01	613.64	29.86	1629.32	265.54	634.96
Median	133.38	2577.75	880.98	995.28	31.38	2085.49	292.00	890.33	45.32	2168.33	294.10	974.45
Maximum	264.93	3423.28	940.98	1714.65	59.89	2842.77	317.33	1082.66	82.46	2909.32	320.86	1207.27
Geometric Mean	139.37	2529.77	882.62	1043.49	33.37	2046.19	290.38	861.92	46.02	2182.10	293.98	927.52
95% Confidence Interval's Lower Limit	128.80	2415.23	874.73	974.86	31.10	1939.16	285.17	822.49	42.78	2076.25	288.87	884.80
95% Confidence Interval's Upper Limit	161.68	2700.77	891.02	1169.67	37.61	2230.05	296.33	921.50	52.41	2339.04	299.79	993.40

Table A3. Pharmacokinetic parameters V_z/F (relative units), Cl/F (h^{-1}), and MRT (h) for analyzed tissues.

Statistical Parameter	V_z/F (Relative Units)				$Cl/F, h^{-1}$				MRT, h			
	Cardiac	Liver	Plasma	Kidney	Cardiac	Liver	Plasma	Kidney	Cardiac	Liver	Plasma	Kidney
Mean	9.46	1.04	0.90	2.58	29.14	0.58	4.26	1.40	0.38	0.98	0.26	1.41
SD	3.48	0.56	0.15	1.32	7.22	0.10	0.21	0.23	0.14	0.33	0.01	0.71
SE	0.64	0.11	0.03	0.24	1.32	0.02	0.04	0.04	0.03	0.06	0.00	0.13
Minimum	4.08	0.21	0.60	0.88	15.94	0.43	3.90	1.10	0.19	0.48	0.24	0.64
Median	9.16	0.95	0.88	2.47	28.83	0.58	4.25	1.33	0.35	0.90	0.26	1.32
Maximum	20.08	3.18	1.22	7.64	44.07	0.81	4.71	1.97	0.74	2.21	0.28	3.36
Geometric Mean	8.85	0.92	0.89	2.31	28.26	0.58	4.25	1.39	0.35	0.94	0.26	1.26
95% Confidence Interval's Lower Limit	8.16	0.82	0.84	2.09	26.45	0.55	4.18	1.32	0.32	0.85	0.26	1.15
95% Confidence Interval's Upper Limit	10.76	1.26	0.96	3.08	31.84	0.62	4.34	1.49	0.43	1.11	0.26	1.68

The ratios of the drug's exposure to tissues to its exposure to the blood plasma of the mice were 0.12, 7.17, and 3.00 for myocardium, liver, and kidney tissues, respectively.

The maximum concentration level in the myocardium tissue coincides temporally with the peaks for the plasma.

At the same time, the time at which the drug's concentration reaches the maximum levels in the liver and kidney tissues significantly lags behind the peak concentration in the blood, which means that the drug transfers to these organs and, thus, allows the assumption of the affinity of the drug molecules to some extracellular or intracellular structures in these organs.

References

1. Bagrov, A.Y.; Shapiro, J.I.; Fedorova, O.V. Endogenous cardiotoxic steroids: Physiology, pharmacology, and novel therapeutic targets. *Pharmacol. Rev.* **2009**, *61*, 9–38. [CrossRef]
2. Pavlovic, D. Endogenous cardiotoxic steroids and cardiovascular disease, where to next? *Cell Calcium* **2020**, *86*, 102156. [CrossRef]
3. Lopachev, A.V.; Lopacheva, O.M.; Osipova, E.A.; Vladychenskaya, E.A.; Smolyaninova, L.V.; Fedorova, T.N.; Koroleva, O.V.; Akkuratov, E.E. Ouabain-induced changes in MAP kinase phosphorylation in primary culture of rat cerebellar cells. *Cell Biochem. Funct.* **2016**, *34*, 367–377. [CrossRef]
4. Neves, C.H.; Tibana, R.A.; Prestes, J.; Voltarelli, F.A.; Aguiar, A.F.; Mota, G.A.F.; de Sousa, S.L.B.; Leopoldo, A.S.; Leopoldo, A.P.L.; Mueller, A.; et al. Digoxin Induces Cardiac Hypertrophy without Negative Effects on Cardiac Function and Physical Performance in Trained Normotensive Rats. *Int. J. Sports Med.* **2017**, *38*, 263–269. [CrossRef] [PubMed]
5. Marck, P.V.; Pessoa, M.T.; Xu, Y.; Kutz, L.C.; Collins, D.M.; Yan, Y.; King, C.; Wang, X.; Duan, Q.; Cai, L.; et al. Cardiac Oxidative Signaling and Physiological Hypertrophy in the Na/K-ATPase $\alpha 1s/\alpha 2s/s$ Mouse Model of High Affinity for Cardiotoxic Steroids. *Int. J. Mol. Sci.* **2021**, *22*, 3462. [CrossRef]
6. Kapelios, C.J.; Lund, L.H.; Benson, L.; Dahlström, U.; Rosano, G.M.C.; Hauptman, P.J.; Savarese, G. Digoxin use in contemporary heart failure with reduced ejection fraction: An analysis from the Swedish Heart Failure Registry. *Eur. Heart J. Cardiovasc. Pharmacother.* **2022**, *8*, 756–767. [CrossRef] [PubMed]
7. El-Mallakh, R.S.; Hedges, S.; Casey, D. Digoxin encephalopathy presenting as mood disturbance. *J. Clin. Psychopharmacol.* **1995**, *15*, 82–83. [CrossRef] [PubMed]
8. Shear, M.K.; Sacks, M. Digitalis delirium: Psychiatric considerations. *Int. J. Psychiatry Med.* **1977**, *8*, 371–381. [CrossRef]
9. El-Mallakh, R.S.; Harrison, L.T.; Li, R.; Changaris, D.G.; Levy, R.S. An animal model for mania: Preliminary results. *Prog. Neuropsychopharmacol. Biol. Psychiatry* **1995**, *19*, 955–962. [CrossRef]
10. Lopachev, A.; Volnova, A.; Evdokimenko, A.; Abaimov, D.; Timoshina, Y.; Kazanskaya, R.; Lopacheva, O.; Deal, A.; Budygin, E.; Fedorova, T.; et al. Intracerebroventricular injection of ouabain causes mania-like behavior in mice through D2 receptor activation. *Sci. Rep.* **2019**, *9*, 15627. [CrossRef]
11. Marchetti, G.V.; Marzo, A.; De Ponti, C.; Scalvini, A.; Merlo, L.; Nosedà, V. Blood levels and tissue distribution of 3 H-ouabain administered per os. An experimental and clinical study. *Arzneimittelforschung* **1971**, *21*, 1399–1403. Available online: <https://www.ncbi.nlm.nih.gov/pubmed/5171797> (accessed on 1 February 2024). [PubMed]
12. Greeff, K.; Köhler, E.; Strobach, H.; Verspohl, E. Zur Pharmakokinetik des g-Strophanthins. In *Verhandlungen Der Deutschen Gesellschaft für Kreislaufforschung*; Steinkopff: Heidelberg, Germany, 1974; pp. 301–305. [CrossRef]
13. Selden, R.; Smith, T.W. Ouabain pharmacokinetics in dog and man. Determination by radioimmunoassay. *Circulation* **1972**, *45*, 1176–1182. [CrossRef] [PubMed]
14. Kawahara, M.; Sakata, A.; Miyashita, T.; Tamai, I.; Tsuji, A. Physiologically based pharmacokinetics of digoxin in *mdr1a* knockout mice. *J. Pharm. Sci.* **1999**, *88*, 1281–1287. [CrossRef] [PubMed]
15. Cooke, D.M. The use of central nervous system manifestations in the early detection of digitalis toxicity. *Heart Lung.* **1993**, *22*, 477–481. Available online: <https://www.ncbi.nlm.nih.gov/pubmed/8288449> (accessed on 1 February 2024). [PubMed]
16. Andersson, K.E.; Bertler, A.; Wettrell, G. Post-mortem distribution and tissue concentrations of digoxin in infants and adults. *Acta Paediatr. Scand.* **1975**, *64*, 497–504. [CrossRef] [PubMed]
17. Keller, S.; Frishman, W.H. Neuropsychiatric effects of cardiovascular drug therapy. *Cardiol. Rev.* **2003**, *11*, 73–93. [CrossRef]
18. Dutta, S.; Marks, B.H.; Schoener, E.P. Accumulation of radioactive cardiac glycosides by various brain regions in relation to the dysrhythmogenic effect. *Br. J. Pharmacol.* **1977**, *59*, 101–106. [CrossRef]
19. Lingrel, J.B.; Croyle, M.L.; Woo, A.L.; Argüello, J.M. Ligand binding sites of Na,K-ATPase. *Acta Physiol. Scand. Suppl.* **1998**, *643*, 69–77. Available online: <https://www.ncbi.nlm.nih.gov/pubmed/9789548> (accessed on 1 February 2024).
20. Jahrmärker, H. *Digitalistherapie: Beiträge zur Pharmakologie und Klinik*; Springer: Berlin/Heidelberg, Germany, 2013; Available online: <https://play.google.com/store/books/details?id=y0CpBgAAQBAJ> (accessed on 1 February 2024).
21. Russell, J.Q.; Klaassen, C.D. Species variation in the biliary excretion of ouabain. *J. Pharmacol. Exp. Ther.* **1972**, *183*, 513–519. Available online: <https://www.ncbi.nlm.nih.gov/pubmed/4636390> (accessed on 1 February 2024).
22. Cohn, K.E.; Kleiger, R.E.; Harrison, D.C. Influence of potassium depletion on myocardial concentration of tritiated digoxin. *Circ Res.* **1967**, *20*, 473–476. [CrossRef]

23. Wu, J.; Li, D.; Du, L.; Baldawi, M.; Gable, M.E.; Askari, A.; Liu, L. Ouabain prevents pathological cardiac hypertrophy and heart failure through activation of phosphoinositide 3-kinase α in mouse. *Cell Biosci.* **2015**, *5*, 64. [CrossRef] [PubMed]
24. Deisl, C.; Fine, M.; Moe, O.W.; Hilgemann, D.W. Hypertrophy of human embryonic stem cell-derived cardiomyocytes supported by positive feedback between Ca and diacylglycerol signals. *Pflugers Arch.* **2019**, *471*, 1143–1157. [CrossRef] [PubMed]
25. Farah, A. Lethal dose and average rate of uptake of g-strophanthin in the heart-lung preparation of the dog under varying conditions. *J. Pharmacol. Exp. Ther.* **1946**, *87*, 364–374. Available online: <https://www.ncbi.nlm.nih.gov/pubmed/20279256> (accessed on 1 February 2024).
26. Kupferberg, H.J.; Schankl, L.S. Biliary secretion of ouabain-3H and its uptake by liver slices in the rat. *Am. J. Physiol.* **1968**, *214*, 1048–1053. [CrossRef] [PubMed]
27. Osol, A. *Remington's Pharmaceutical Sciences*, 16th ed.; Mack Publishing Company: London, UK, 1980.
28. Zhang, D.; Wei, C.; Hop, C.E.C.A.; Wright, M.R.; Hu, M.; Lai, Y.; Khojasteh, S.C.; Humphreys, W.G. Intestinal Excretion, Intestinal Recirculation, and Renal Tubule Reabsorption Are Underappreciated Mechanisms That Drive the Distribution and Pharmacokinetic Behavior of Small Molecule Drugs. *J. Med. Chem.* **2021**, *64*, 7045–7059. [CrossRef]
29. Steiness, E. Renal tubular secretion of digoxin. *Circulation* **1974**, *50*, 103–107. [CrossRef] [PubMed]
30. Roman, R.J.; Kauker, M.L. Renal tubular transport of 3H-digoxin in saline diuresis in rats. *Circ. Res.* **1976**, *38*, 185–191. [CrossRef] [PubMed]
31. Li, C.; Liang, D.; Liu, Y.; Shen, C.; Wang, X.; Yang, B.; Li, X.; Wang, W.; Xu, M.; Pu, Z.; et al. Evaluation of the Influence of Zhenwu Tang on the Pharmacokinetics of Digoxin in Rats Using HPLC-MS/MS. *Evid. Based Complement. Altern. Med.* **2021**, *2021*, 2673183. [CrossRef]
32. Forrest, A.B.; Hawley, J.C.; Malone, M.H. Testing for circadian differences in lethality for intravenous ouabain in male mice. *J. Ethnopharmacol.* **1993**, *39*, 161–166. [CrossRef]
33. Erdle, H.P.; Schultz, K.D.; Wetzell, E.; Gross, F. Resorption und Ausscheidung von g-Strophanthin nach intravenöser und perlingualer Gabe [Absorption and excretion of g-strophanthin after intravenous or sublingual administration (author's transl)]. *Dtsch. Med. Wochenschr.* **1979**, *104*, 976–979, In German. [CrossRef]
34. Manfred, D. May Strophanthin Be a Valuable Cardiac drug? *Am. J. Med. Clin. Res. Rev.* **2023**, *2*, 1–6. [CrossRef]
35. Shevchenko, V.P.; Nagaev, I.Y.; Lopachev, A.V.; Myasoedov, N.F. Synthesis of Deuterium-Labeled Ouabain—an Internal Standard in Toxicological and Pharmacological Studies. *Pharm. Chem. J.* **2023**, *56*, 1491–1495. [CrossRef]
36. Miroshnichenko, I.; Simonov, A.N.; Kuzmin, I.I.; Platova, A.I. Analysis of sparse data in pharmacokinetic studies. *Pharmacokinet. Pharmacodyn.* **2020**, *2*, 28–33. [CrossRef]

Disclaimer/Publisher's Note: The statements, opinions and data contained in all publications are solely those of the individual author(s) and contributor(s) and not of MDPI and/or the editor(s). MDPI and/or the editor(s) disclaim responsibility for any injury to people or property resulting from any ideas, methods, instructions or products referred to in the content.